JOURNAL OF MOLECULAR SPECTROSCOPY 155, 315–325 (1992)

Fourier Transform Infrared Emission Spectroscopy of a New $A\,^3\Pi_i - X\,^3\Sigma^-$ System of NiO

R. S. RAM AND P. F. BERNATH[1,2]

Department of Chemistry, University of Arizona, Tucson, Arizona 85721

A new $A\,^3\Pi_i - X\,^3\Sigma^-$ electronic transition of NiO has been observed in the near infrared region extending from 2.1 to 2.6 μm. The molecule was excited in emission from an Ni hollow cathode discharge and the spectra were observed using a Fourier transform spectrometer. The observed spectrum consists of the 0–0 band for the $^3\Pi_0 - ^3\Sigma_1^-$, $^3\Pi_1 - ^3\Sigma_0^-$ subbands and the 1–1 band of the $^3\Pi_1 - ^3\Sigma_0^-$ subband. The subbands involving $^3\Pi_2$ spin component were not observed. The molecular constants including the Λ-doubling constants in the excited $A\,^3\Pi_i$ state have been determined. The principal constants for the new excited state obtained from this analysis are $T_0 = 4337.5554(12)$ cm^{-1}, $A_0 = -283.3713(16)$ cm^{-1}, and $B_0 = 0.494659(11)$ cm^{-1}.

INTRODUCTION

Diatomic transition-metal oxides are found in the atmospheres of cool stars (*1*). For example TiO and VO were identified in the spectra of M-type stars and are used by astronomers in stellar classification (*2*). The diatomic transition metal oxides also provide simple models for bonding which can be applied, for example, to the study of oxide binding to catalytic metal surfaces. As a result of this interest there has been much recent work on diatomic transition–metal oxides (for example, Refs. *3–9*).

Although some high-resolution work is available for all of the 3*d* metal monoxides (*4*), the data for NiO are particularly sparse. The first spectrum of NiO was observed in the visible region (400–900 nm) by Rosen (*10*). Rosen's bands were not rotationally analyzed because they were very complex and perturbed. Green *et al.* (*11*) recorded the infrared spectrum of matrix isolated NiO and found $\omega_e = 838$ cm^{-1} and $\omega_e x_e = 5.9$ cm^{-1}. The visible NiO bands were also observed, but not analyzed, by Gustafsson and Scullman (*12*) as well as McQuaid *et al.* (*13*).

The spectra of transition metal oxides are usually very complex because of the presence of a large number of states derived from several low-lying configurations. The open *d*-shell gives rise to states with large multiplicities and large orbital angular momenta, which are split by substantial spin–orbit interactions. The many states and spin components perturb each other and provide impressively complex visible spectra. As a result of these problems, the first rotational analysis of NiO was not carried out until 1988 (*9*). Srdanov and Harris (*9*) used laser techniques to analyze several bands in the green region of the spectrum. As is often the case for transition-metal oxides, they were not able to provide a definitive characterization of the perturbed upper states, but they provided excellent ground state constants (*9*).

Fortunately there are several ab initio calculations of the electronic structure of NiO (*14–17*). These calculations (*14–16*) predict a $^3\Sigma^-$ ground state with a low lying

[1] Also: Department of Chemistry, University of Waterloo, Waterloo, Ontario, Canada N2L 3G1.
[2] Camille and Henry Dreyfus Teacher-Scholar.

0022-2852/92 $5.00

$^3\Pi$ state. In this paper we report the observation of the $A^3\Pi$–$X^3\Sigma^-$ infrared electronic transition of NiO between 3850 and 4650 cm^{-1}.

The $A^3\Pi$ state is found to be free of local perturbations, although there is evidence of substantial global interaction with other states. Although the visible transitions of transition-metal oxides have strongly perturbed excited states, the infrared transitions are expected to be relatively unperturbed because of the decrease in the density of excited states.

After our work on NiO was completed we learned of the work of Friedman-Hill and Field (*18*) who observed the $A^3\Pi$ state by dispersing laser-induced fluorescence with a monochromator. In their work a $^3\Sigma^-$–$X^3\Sigma^-$ transition was excited near 620 nm and fluorescence into the $A^3\Pi$ state was observed at 790 nm.

EXPERIMENTAL DETAILS

The NiO molecules were made in a hollow cathode discharge lamp. A mixture of 3.8 Torr of Ne and 0.2 Torr of O_2 flowed through a nickel cathode. The lamp was operated at 340 V and 320 mA current.

The emission from NiO was observed with the Fourier transform spectrometer associated the McMath Solar telescope of the National Solar Observatory at Kitt Peak. The spectrometer was operated with liquid-N_2-cooled InSb detectors and a CaF_2 beamsplitter. The detector response and an Si filter restricted the spectrometer band pass to the 1800–9000 cm^{-1} region. A total of nine scans were co-added in 1 hr of integration at an unapodized resolution of 0.02 cm^{-1}.

The observed spectrum contains the atomic lines of Ne and Ni as well as the vibration–rotation bands of CO and the $A^3\Pi$–$X^3\Sigma^-$ transition of NiO. The fundamental vibration–rotation band of CO (*19*) was used for the calibration of the spectrum of NiO. The absolute accuracy of the data is estimated to be better than ± 0.001 cm^{-1} for strong unblended lines. However, most lines are relatively weak with a typical measurement accuracy of ± 0.003 cm^{-1}.

OBSERVATIONS AND ANALYSIS

The spectral reduction program, PC-DECOMP, developed by J. Brault, was used in the data reduction and transition wavenumber determination. The peak positions were determined by fitting a Voigt lineshape function to each observed spectral feature.

The new NiO bands lie in the 3850–4650 cm^{-1} region. The most intense feature at 4382.1 cm^{-1} has been identified as the $^3\Pi_1$–$^3\Sigma_0^-$ subband. This band consists of three branches: P, Q, and R. The lower-state combination differences match, to within experimental error, the values given by Srdanov and Harris (*9*) for the $v'' = 0$, $^3\Sigma_0^-$ substate of NiO. On the higher wavenumber side of this band, there are two bandheads at 4575 and 4635 cm^{-1}. These have been identified as the 0–0 band of $^3\Pi_0$–$^3\Sigma_1^-$ subband. The lower state combination differences in this subband match with the $v'' = 0$, $^3\Sigma_1^-$ combination differences of Srdanov and Harris (*9*).

On the lower wavenumber side of the 0–0 $^3\Pi_1$–$^3\Sigma_0^-$ subband, there are three relatively weak bandheads at 4321.5, 4259.7, and 4196.9 cm^{-1}, with the same appearance as the 0–0 $^3\Pi_1$–$^3\Sigma_{0^+}^-$ subband. The consecutive spacing between these heads is 60.6, 61.8, and 62.8 cm^{-1}. This suggests that these three bands are most probably the 1–1, 2–2, and 3–3 bands of the $^3\Pi_1$–$^3\Sigma_{0^+}^-$ subband.

In the present analysis we have measured the 0–0 band of the $^3\Pi_1$–$^3\Sigma_{0^+}^-$, $^3\Pi_{0^+}$–$^3\Sigma_1^-$, and $^3\Pi_0$–$^3\Sigma_1^-$ subbands and the 1–1 band of the $^3\Pi_1$–$^3\Sigma_{0^+}^-$ subband each

consisting of three branches, P, Q, and R. The observed transition wavenumbers were fitted with the usual N^2 Hamiltonian for the $^3\Pi$ and $^3\Sigma$ states as given by Brown *et al.* (*20*). An explicit list of the matrix elements is provided by Brazier *et al.* (*21*). The R branch in the $^3\Pi_0$–$^3\Sigma_1^-$ subband was too weak to be measured, so the J-assignment in the P and Q branches was accomplished by adjusting J in these branches and minimizing the standard deviation of the fit.

The $^3\Pi_2$–$^3\Sigma_1$ subband was the weakest of the three possible subbands $^3\Pi_1$–$^3\Sigma_{0^+}^-$, $^3\Pi_0$–$^3\Sigma_1^-$, and $^3\Pi_2$–$^3\Sigma_1^-$. We could not identify this subband with any certainty in our spectra. We observed some weak lines of a branch in the 3885–3900 cm^{-1} region, but a definite assignment was not possible.

The relative intensity of the various subbands should be determined by the Hund's case (a) selection rule $\Delta\Sigma = 0$. The $X^3\Sigma^-$ has considerable case (a) character because the $^3\Sigma_1^-$ and $^3\Sigma_{0^+}^-$ components are separated by $2\lambda = 50$ cm^{-1}. The $^3\Pi_{0^+}$ and $^3\Pi_{0^-}$ spin components have $\Lambda = \pm 1$ and $\Sigma = \mp 1$ so the $^3\Pi_{0^+}$–$^3\Sigma_1^-$ and $^3\Pi_{0^-}$–$^3\Sigma_1^-$ subbands should be strong. For $^3\Pi_1$, $\Lambda = \mp 1$ and $\Sigma = 0$ so the $^3\Pi_1$–$^3\Sigma_{0^+}^-$ subband is expected to be strong. Finally, $^3\Pi_2$ has $\Lambda = \pm 1$ and $\Sigma = \pm 1$ so the $^3\Pi_2$–$^3\Sigma_1$ subband should be observable. A more detailed calculation of the intensity factors confirms these predictions and sheds no light on the observed weakness of the $^3\Pi_2$–$^3\Sigma_1$ subband. Presumably the $A^3\Pi$ state has considerable Hund's case (c) character, as evidenced by the large $^3\Pi_{0^+}$–$^3\Pi_{0^-}$ splitting (~ -60 cm^{-1}), so an intensity calculation based on a single unmixed excited $^3\Pi$ state is unreliable.

The ab initio calculations of Walch and Goddard (*14*) predict a $^1\Delta_2$ near the $A^3\Pi$ state. Mixing of the $A^3\Pi_2$ spin component with the $^1\Delta_2$ state would weaken the $A^3\Pi_2$–$X^3\Sigma_1^-$ transition. The predicted position of the origin of the $A^3\Pi_2$–$X^3\Sigma_1$ subband on the basis of the constants derived from the other spin components is 4035 cm^{-1}. The very weak lines near 3900 cm^{-1} are consistent with a nearby $^1\Delta_2$ state lying above the $^3\Pi_2$ spin component and shifting it to lower energy.

Our final fits included the ground state combination differences of Srdanov and Harris (*9*). The molecular parameters T_0, A_0, A_{D0}, B_0, D_0, q_0, q_{D0}, p_0, p_{D0} in the excited state and B_0, D_0, γ_0, γ_{D0}, γ_0, and γ_{D0} in the ground state were varied for the 0–0 band. The exclusion of the $^3\Pi_2$–$^3\Sigma_1$ subband in the fit prevents the determination of the spin–spin constant λ in the $A^3\Pi$ state. This parameter is expected to be large because of the Hund's case (c) tendencies of the $A^3\Pi$ state but is highly correlated with the constants T_0 and A_0. Therefore the values of T_0 and A_0 obtained from our analysis are only effective values which reproduce the data.

No direct transitions were observed which connect the $^3\Sigma_{0^+}^-$ and $^3\Sigma_1^-$ spin components in the ground state. The ground state λ and λ_D values were determined indirectly in the fits from the effects of spin uncoupling and are, therefore, not very reliable. The small statistical errors for many of the parameters in Table II are misleading, since they do not include the errors introduced by correlations among the parameters.

The analysis of the 1–1 band was more difficult than the 0–0 band because of the observation of only the $^3\Pi_1$–$^3\Sigma_{0^+}^-$ subband. In this subband the P branch was very weak in intensity and could not be picked out with certainty. For the 1–1 band fit, B_1, D_1, and γ_1 in the ground state as well as T_1, B_1, D_1, and q_1 in the excited state were varied. The other constants were held fixed to the corresponding values obtained from the 0–0 band fit. The ground state combination differences of Srdanov and Harris (*9*) for $v = 1$, $^3\Sigma_1^-$ were also included in the final fit. The observed transition wavenumbers of NiO are given in Table I and the molecular constants obtained in the final fits are provided in Tables II and III.

TABLE I

Observed Transition Wavenumbers (in cm^{-1}) of the $A^3\Pi_i$–$X^3\Sigma^-$ System of NiO

	0-0 $^3\Pi_1$ - $^3\Sigma_0^-$					
J	R_{ee}	O-C	Q_{fe}	O-C	P_{ee}	O-C
2	4373.4242	0.0043				
3						
4	4375.7026	0.0008				
5			4370.8983	0.0039		
6	4378.1416	0.0024	4371.1173	0.0011	4365.2608	0.0049
7			4371.3680	-0.0002	4364.5448	-0.0010
8	4380.7177	0.0044	4371.6500	0.0022	4363.8666	-0.0010
9	4382.0488	0.0039	4371.9514	-0.0011	4363.2208	0.0024
10	4383.4059	0.0034	4372.2811	0.0021	4362.5976	0.0020
11	4384.7783	-0.0047	4372.6205	-0.0042	4361.9937	-0.0025
12	4386.1817	-0.0020	4372.9853	-0.0015	4361.4173	0.0001
13	4387.6006	-0.0012	4373.3647	0.0022	4360.8545	-0.0018
14	4389.0345	0.0000	4373.7491	0.0001	4360.3083	-0.0022
15	4390.4762	-0.0031	4374.1413	-0.0026	4359.7765	-0.0009
16	4391.9322	-0.0017	4374.5417	-0.0031	4359.2547	0.0002
17	4393.3899	-0.0059	4374.9474	-0.0020	4358.7389	-0.0008
18	4394.8612	-0.0015	4375.3515	-0.0040	4358.2282	-0.0025
19	4396.3262	-0.0068	4375.7656	0.0044	4357.7233	-0.0023
20	4397.8091	0.0045	4376.1685	0.0039	4357.2283	0.0057
21	4399.2721	-0.0036	4376.5690	0.0050	4356.7182	-0.0017
22	4400.7410	-0.0037	4376.9627	0.0049	4356.2146	-0.0014
23	4402.2058	-0.0045	4377.3456	0.0010	4355.7184	0.0090
24	4403.6679	-0.0029	4377.7234	0.0005	4355.1971	-0.0017
25	4405.1220	-0.0031	4378.0912	-0.0005	4354.6918	0.0089
26			4378.4494	-0.0002	4354.1630	0.0024
27	4408.0079	-0.0025	4378.7936	-0.0021	4353.6302	-0.0005
28	4409.4421	0.0029	4379.1249	-0.0040	4353.0910	-0.0015
29	4410.8550	-0.0026	4379.4441	-0.0043	4352.5486	0.0037
30	4412.2659	0.0012	4379.7513	-0.0020	4351.9830	-0.0040
31	4413.6628	0.0032	4380.0432	0.0004	4351.4157	-0.0025
32	4415.0415	-0.0002	4380.3166	0.0003	4350.8366	-0.0012
33	4416.4109	0.0007	4380.5625	-0.0106	4350.2477	0.0028
34	4417.7635	-0.0009	4380.8145	0.0020	4349.6400	0.0008
35	4419.1054	0.0016	4381.0363	0.0023	4349.0207	0.0007
36	4420.4256	-0.0021	4381.2330	-0.0041		
37			4381.4212	-0.0002		
38	4423.0298	0.0027	4381.5868	0.0007		
39	4424.3089	0.0072	4381.7291	-0.0020		
40	4425.5565	-0.0025	4381.8562	0.0004		
41			4381.9543	-0.0056		
42			4382.0488	0.0057		
43	4429.2198	-0.0026	4382.1041	-0.0009		
44	4430.4054	-0.0008	4382.1496	0.0044		
45	4431.5672	-0.0035				

DISCUSSION

We present the first observation of the $A^3\Pi_i$–$X^3\Sigma^-$ transition of NiO. The rotational analysis of the 0–0 band and 1–1 bands provides the equilibrium rotational constants (Table IV) of this molecule. The observed bond lengths in the ground and excited states are found to be 1.64489 and 1.62712 Å.

The ground state vibrational constants of NiO, as reported by Srdanov and Harris (*9*) are ω_e = 839.1 cm^{-1} and $\omega_e x_e$ = 5.4 cm^{-1}. Using the values of the band origins of the 0–0 and 1–1 bands the value of $\Delta G'_{1/2}$ = 769.0 cm^{-1} is obtained. From the intervals between the 0–0, 1–1, 2–2, and 3–3 heads the value of $\omega'_e x'_e$ = 5.9 cm^{-1} is deduced, giving ω'_e = 780.8 cm^{-1}. These values need to be used carefully since data for only the $^2\Pi_1$–$^3\Sigma_{0^+}$ subband was used for the 1–1 transition. Since the $A^3\Pi$ state has considerable case (c) character, different effective vibrational frequencies are possible for each spin component.

TABLE I—*Continued*

	0-0 $^3\Pi_{0^-}$ - $^3\Sigma_1^-$					
J	R_{ff}	O-C	Q_{fe}	O-C	P_{ff}	O-C
3			4574.9709	-0.0007		
4			4574.6646	0.0090		
5	4581.1878	0.0036				
6			4573.7996	-0.0001		
7	4582.9673	0.0004	4573.2656	0.0013	4568.0346	0.0007
8			4572.6628	0.0022		
9			4571.9680	-0.0036	4565.7670	-0.0048
10			4571.2609	0.0010	4564.6167	-0.0002
11					4563.4288	-0.0173
12			4569.6226	0.0027		
13	4587.9332	0.0084	4568.7231	0.0061		
14			4567.7848	0.0022	4559.8306	-0.0076
15	4589.4436	-0.0026	4566.7562	-0.0027		
16	4590.1813	-0.0008	4565.7083	-0.0002	4557.3496	-0.0037
17	4590.8986	-0.0027	4564.6167	0.0033	4556.0752	-0.0117
18	4591.5983	-0.0055	4563.4736	-0.0023	4554.7986	-0.0060
19			4562.2971	-0.0005	4553.5060	-0.0001
20			4561.0752	-0.0055	4552.1950	0.0033
21	4593.6030	-0.0077	4559.8306	0.0041		
22	4594.2320	-0.0139	4558.5358	-0.0010	4549.5143	-0.0003
23	4594.8637	-0.0002	4557.2124	-0.0003	4548.1541	0.0022
24	4595.4682	0.0033	4555.8580	0.0024	4546.7733	0.0002
25	4596.0482	-0.0005	4554.4674	0.0006	4545.3844	0.0064
26	4596.6142	-0.0011	4553.0462	-0.0010	4543.9720	0.0053
27	4597.1668	0.0023	4551.5976	-0.0002	4542.5294	-0.0097
28	4597.6838	-0.0126	4550.1176	-0.0020	4541.1006	0.0054
29	4598.2145	0.0038	4548.6154	0.0021	4539.6342	-0.0007
30	4598.7048	-0.0026	4547.0804	0.0008	4538.1691	0.0108
31			4545.5179	-0.0015		
32	4599.6533	0.0056	4543.9317	-0.0013		
33			4542.3180	-0.0031	4533.6365	0.0071
34	4600.5180	0.0013	4540.6839	-0.0003	4532.0904	0.0038
35			4539.0182	-0.0046	4530.5251	-0.0021
36			4537.3358	-0.0015		
37	4601.6768	-0.0075	4535.6257	-0.0024	4527.3600	0.0021
38	4602.0394	0.0026	4533.8946	-0.0008	4525.7472	-0.0009
39	4602.3660	-0.0050	4532.1403	0.0008		
40	4602.6801	-0.0064	4530.3611	0.0002		
41	4602.9848	0.0014	4528.5587	-0.0010	4520.8162	-0.0004
42			4526.7389	0.0028		
43					4517.4443	0.0010
44					4515.7330	0.0022
45						
46			4519.2336	0.0119	4512.2555	0.0019
47			4517.2933	0.0045	4510.4934	0.0048
48						
49			4513.3642	0.0057	4506.9010	-0.0049
50			4511.3594	-0.0021		
51					4503.2455	-0.0065
52						
53			4505.2429	0.0003		
54			4503.1422	-0.0184		
55			4501.0582	0.0007		

An overview of the $A^3\Pi$–$A^3\Sigma^-$ transition is provided in Fig. 1, while a section of the 0–0 band of the $^3\Pi_1$–$^3\Sigma_{0^+}^-$ subband is presented in Fig. 2, where the lines belonging to the main isotopomer, ^{58}NiO, have been marked. Ni has five naturally occuring isotopes, ^{58}Ni, ^{60}Ni, ^{61}Ni, ^{62}Ni and ^{65}Ni, present with abundances of 68.27, 26.10, 1.13, 3.59, and 0.91%, respectively. The intensity the second most abundant isotopomer, ^{60}NiO, is expected to be ~38% of ^{58}NiO. The lines belonging to ^{60}NiO could be picked out in certain regions, but there was insufficient data for an independent analysis of the minor isotope. However, the observation of some lines due to ^{60}NiO does confirm the vibrational assignment.

The bonding in NiO can be rationalized (*14–16*) by considering the $A^3\Pi$ and $X^3\Sigma^-$ states to arise from the ionic Ni^+O^- structure. Ni^+O^- has a $3d^9$ atomic configuration

TABLE I—*Continued*

	0-0 $^3\Pi_{0^+}$ - $^3\Sigma^-$				1-1 $^3\Pi_1$ - $^3\Sigma_0^-$			
J	Q_{ef}	O-C	P_{ee}	O-C	R_{ee}	O-C	Q_{fe}	O-C
4	4634.4628	0.0022						
5	4634.3743	0.0047	4628.4512	-0.0050				
6	4634.2458	-0.0146	4626.9936	0.0086				
7	4634.1301	-0.0029					4312.0321	-0.0022
8	4633.9870	-0.0004					4312.3033	0.0038
9	4633.8180	-0.0056	4622.1418	-0.0033			4312.5904	0.0024
10	4633.6405	-0.0009					4312.8968	-0.0003
11	4633.4479	0.0069	4618.5871	-0.0034			4313.2126	-0.0113
12	4633.2206	-0.0017	4616.7167	-0.0067			4313.5639	-0.0018
13	4632.9834	-0.0019						
14	4632.7346	0.0047	4612.8245	0.0015	4329.4373	0.0052	4314.2768	-0.0066
15	4632.4584	0.0024	4610.7943	-0.0007	4330.8475	0.0032	4314.6553	0.0010
16	4632.1584	-0.0056	4608.7175	-0.0009	4332.2698	0.0047	4315.0291	-0.0008
17	4631.8486	-0.0048	4606.5958	0.0005	4333.6909	-0.0012	4315.4105	0.0024
18	4631.5221	-0.0023			4335.1327	0.0092	4315.7870	0.0003
19	4631.1747	-0.0022	4602.2229	0.0047	4336.5554	-0.0015	4316.1648	0.0009
20	4630.8111	0.0002	4599.9752	0.0072	4337.9862	-0.0045	4316.5335	-0.0042
21	4630.4269	0.0006	4597.6838	0.0050	4339.4171	-0.0059	4316.9025	-0.0039
22	4630.0200	-0.0033	4595.3583	0.0059	4340.8538	0.0014	4317.2646	-0.0040
23	4629.6002	-0.0013	4592.9875	-0.0026	4342.2774	0.0001	4317.6250	0.0023
24			4590.5882	-0.0050	4343.6921	-0.0042	4317.9657	-0.0018
25			4588.1617	-0.0012	4345.0988	-0.0095	4318.3006	-0.0011
26	4628.2244	0.0003	4585.7042	0.0038	4346.5135	0.0016	4318.6219	-0.0023
27	4627.7285	0.0011	4583.2120	0.0054	4347.9110	0.0048	4318.9390	0.0052
28	4627.2119	-0.0001			4349.2929	0.0028	4319.2303	0.0007
29	4626.6782	0.0006						
30	4626.1221	-0.0021	4575.5414	-0.0051			4319.7773	0.0007
31	4625.5545	0.0025	4572.9334	-0.0028			4320.0304	0.0042
32	4624.9610	0.0004	4570.3021	0.0036			4320.2631	0.0043
33	4624.3521	0.0019					4320.4725	-0.0013
34	4623.7250	0.0044	4564.9369	-0.0063			4320.6737	0.0031
35	4623.0736	0.0018					4320.8511	0.0024
36	4622.4054	0.0016					4321.0039	-0.0036
37	4621.7175	0.0011	4556.7136	-0.0050			4321.1421	-0.0044
38	4621.0104	0.0008	4553.9293	0.0018				
39	4620.2853	0.0020						
40	4619.5421	0.0045	4548.2646	-0.0087				
41	4618.7706	-0.0017	4545.3844	-0.0263				
42	4617.9928	0.0056	4542.5294	0.0045				
43	4617.1827	0.0003	4539.6342	0.0182				
44	4616.3563	-0.0015						
45	4615.5042	-0.0093	4533.7322	0.0022				
46	4614.6558	0.0068						
47	4613.7623	-0.0023						
48	4612.8248	-0.0352						
49	4611.9279	-0.0073						
50	4610.9934	0.0033						

for Ni^+ and a $2p^5$ configuration for O^-. In a linear molecule the $3d$ hole on Ni^+ can be $3d\delta^{-1}$, $3d\pi^{-1}$, and $3d\sigma^{-1}$, while O^- has $2p\pi^{-1}$ and $2p\sigma^{-1}$ holes. Ab initio calculations (*14–16*) predict that the ground $X^3\Sigma^-$ state arises principally from coupling the $3d\pi^{-1}$ hole on Ni^+ with the $2p\pi^{-1}$ hole on O^-. The first excited state is predicted by Bauschlicher *et al.* (*15*) to be the $A^3\Pi$ state at 4180 cm^{-1} arising from the $Ni^+ 3d\sigma^{-1}$, $O^- 2p\pi^{-1}$ configuration.

Walch and Goddard (*14*) predict that the first excited state of NiO is $^1\Delta$ rather than $^3\Pi$, and they place the $^3\Pi$ state at about 6000 cm^{-1} above the $X^3\Sigma^-$ state. In a slightly more recent calculation (multireference configuration interaction, MRCI), Bauschlicher (*16*) places the $A^3\Pi$ state at 3260 cm^{-1} above the $X^3\Sigma^-$ state. The observed $A^3\Pi$–$X^3\Sigma^-$ transition is found at 4330 cm^{-1}, in reasonable agreement with the calculations.

TABLE II

Rotational Constants for the $X^3\Sigma^-$ State of NiO (in cm^{-1})

Constant	v=0	v=1
B_v	0.505823(11)[a]	0.501488(49)
$10^7 x\ D_v$	7.387(47)	7.46(44)
γ_v	-0.239196(53)	-0.2390(13)
$10^6 x\ \gamma_{Dv}$	-1.208(41)	-1.208[b]
λ_v	24.94811(85)	24.94811[b]
$10^5 x\ \lambda_{Dv}$	3.33(15)	3.33[b]

[a] One standard deviation error is given in parentheses.

[b] Fixed at the values for v = 0.

TABLE III

Rotational Constants for the $A^3\Pi_i$ State of NiO (in cm^{-1})

Constant	v=0	v=1
T_{vv}	4337.5554(12)[a]	4278.2746(21)
A_v	-283.3713(16)	-283.3713[b]
$10^4 x\ A_{Dv}$	-8.479(28)	-8.479[b]
B_v	0.494659(11)	0.489829(76)
$10^7 x\ D_v$	7.985(46)	7.94(44)
$10^4 x\ q_v$	-9.454(46)	-9.960(45)
$10^8 x\ q_{Dv}$	-1.35(23)	-1.35[b]
p_v	0.10594(48)	0.10594[b]
$10^7 x\ p_D$	9.1(17)	9.1[b]
o_v	-29.7011(10)	-29.7011[b]

[a] One standard deviation error is given in parentheses.

[b] Fixed at the values for v=0.

TABLE IV

Equilibrium Constants for the $A^3\Pi_i$ and $X^3\Sigma^-$ States of NiO (in cm^{-1})

Constant	$A^3\Pi_i$	$X^3\Sigma^-$
B_e	0.497074(39)	0.507991(27)
α_e	0.004830(76)	0.004335(50)
ω_e	780.8[a]	839.1[b]
$\omega_e x_e$	5.9[a]	5.4[b]
r_e(Å)	1.64489(6)	1.62712(4)

[a] See text for details.

[b] Fixed to the values given by Srdanov and Harris (9).

NiO is isovalent with PtO which also has a $^3\Sigma^-$ state as the ground state. In PtO the spin–spin splitting (due to second-order spin–orbit interactions) is very large compared to that in NiO where $2\lambda = 50\ cm^{-1}$. In fact, the lowest 0^+ and 1 states of PtO, which are split by approximately 946 cm^{-1}, were treated as $^1\Sigma^+$ and $^1\Pi$ states in the initial high-resolution work. In 1983 Sassenberg and Scullman (*22*) noted that the $\Omega = 0^+$ and $\Omega = 1$ states were components of a Hund's case (c) $X^3\Sigma^-$ state. For NiO

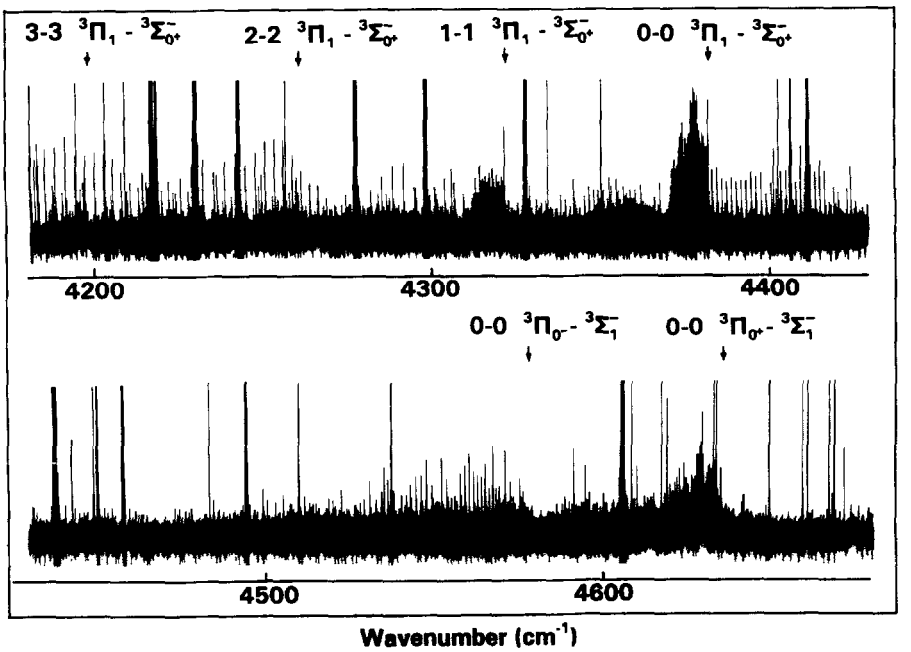

FIG. 1. Overview of the $A^3\Pi$–$X^3\Sigma^-$ transition of NiO.

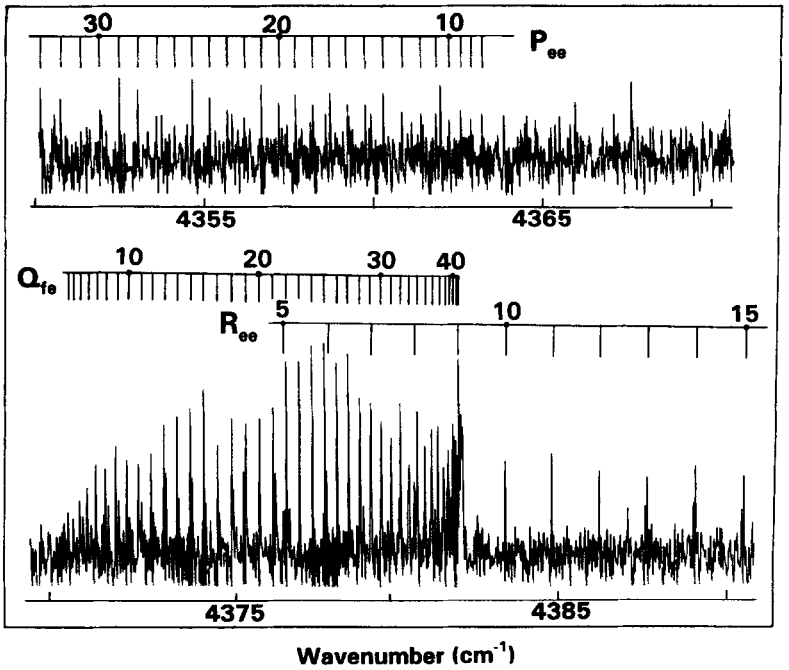

FIG. 2. The 0–0 band of the $A^3\Pi_1$–$X^3\Sigma_{\bar{0}^+}$ subband of NiO.

the ground state, $^3\Sigma^-$, is probably better described as having Hund's case (a) tendencies because both $^3\Sigma_1^-$ and $^3\Sigma_{\bar{0}^+}$ spin components can be fitted together with a single set of effective constants. For PtO, in contrast, the $^3\Sigma_1$ and $^3\Sigma_{0^+}$ components must be fitted separately.

The $A^3\Pi$ state of NiO arises from a configuration (*15*) $\sigma\delta^4\pi^3$ ($Ni^+3d\sigma^{-1}$, $O^-2p\pi^{-1}$) which is greater than half-filled so the $A^3\Pi_i$ state is expected to be inverted. The $^3\Pi_{0^+}$ and $^3\Pi_{0^-}$ components lie above the $^3\Pi_1$ component in agreement with this prediction. The corresponding state in PtO, $A'^3\Pi$, has been located about 8000 cm^{-1} above the $X^3\Sigma^-$ state (*23*). However, the $A'^3\Pi$ state of PtO is a case (c) state and the energy ordering of the spin components is not inverted. No ab initio theoretical calculations are available for PtO.

The simple Ni^+ O^- picture of the bonding in NiO can be tested by assuming that the $A^3\Pi$ and $X^3\Sigma^-$ states form a unique perturber pair. If the configurations of these states differ only in the occupation of Ni^+ $3d$ orbitals (as discussed above) then the pure precession approximation (*24*) with $l = 2$ applies. If instead the $A^3\Pi$ state has an $Ni^+3d\pi^{-1}$, $O^-2p\sigma^{-1}$ configuration then the pure precession approximation applies to the O^-2p orbitals with $l = 1$.

The atomic spin-orbit parameters (ζ) are 672 cm^{-1} for Ni^+ and 121 cm^{-1} for O^{-1} (*24*). In the case of a $^3\Pi$ state from $Ni^+3d\sigma^{-1}$, $O^-2p\pi^{-1}$, $A = -\zeta_{O^-}/2 = -61$ cm^{-1}, while for a $^3\Pi$ state from $Ni^+3d\pi^{-1}$, $O^-2p\sigma^{-1}$, $A = -\zeta_{Ni^+}/2 = -336$ cm^{-1}. The observed value of $A = -283$ cm^{-1} is consistent with a mixed state with a substantial contribution from both these configurations to the $A^3\Pi$ state.

For the $X^3\Sigma^-$ the value of λ can be estimated from the very crude approximation that only the interaction with the $^1\Sigma^+$ state from the same configuration contributes

to the off-diagonal spin–orbit interaction (*24*). Thus the spin splitting $2\lambda \approx (\zeta_{Ni^+})^2/(E(^1\Sigma^+)-E(^3\Sigma^-))$ ignoring the spin–orbit contributions of O^-. Bauschlicher (*16*) calculates that the nearest $^1\Sigma^+$ state is 8340 cm^{-1} above the $X^3\Sigma^-$ state giving $2\lambda \approx 54$ cm^{-1} compared to the observed value of 50 cm^{-1}. This agreement is deceptive because the states in NiO are such a mixture of configurations. For example, the $^1\Sigma^+$ state of Bauschlicher (*16*) is calculated to have nominal $Ni^+ 3d\sigma^{-1}$, $O^- 2p\sigma^{-1}$ character, not the required $Ni^+ 3d\pi^{-1}$, $O^- 2p\pi^{-1}$ character.

The o parameter in the $A^3\Pi$ is difficult to interpret because it has off-diagonal spin–orbit contributions from the $^3\Sigma^-$ state below and the $^1\Sigma^+$ state above in energy. The pure precession values (*21*) for $p = -4AB/(E(^3\Pi)-E(^3\Sigma^-))$ and $q = -4B^2/(E(^3\Pi)-E(^3\Sigma^-))$ are 0.13 cm^{-1} and $-2.3 \times 10^{-4} cm^{-1}$ using $l = 1$. The observed value of p is 0.11 cm^{-1} and of q is -9.5×10^{-4} cm^{-1}, in modest agreement with the simple predictions. Again because of the heavy mixing of configurations, simple models like pure precession are not expected to be very reliable and may be misleading.

CONCLUSION

A new infrared electronic transition of NiO, $A^3\Pi_i$–$X^3\Sigma^-$, was observed by Fourier transform emission spectroscopy of a hollow cathode discharge. The $A^3\Pi$ state is free of local perturbations, although there is evidence of considerable global interaction with other states. Infrared electronic spectroscopy of transition metal oxides promises to be very useful because, in general, the spectra display fewer perturbations than the visible and UV spectra.

ACKNOWLEDGMENTS

We thank J. Wagner, C. Plymate, and G. Ladd for assistance in obtaining the spectra at Kitt Peak. The National Solar Observatory is operated by the Association of Universities for Research in Astronomy, Inc., under contract with the National Science Foundation. We thank M. Dulick for a calculation of the $^3\Pi$–$^3\Sigma^-$ rotational intensity factors. We also thank E. J. Friedman-Hill and R. W. Field for a copy of Ref. (*18*) in advance of publication. Acknowledgment is made to the donors of the Petroleum Research Fund, administered by the ACS, for partial support of this research. Support was also provided by the Center of Excellence in Molecular and Interfacial Dynamics (CEMAID).

RECEIVED: April 6, 1992

REFERENCES

1. H. SPINRAD AND R. F. WING, *Annu. Rev. Astron. Astrophys.* **7**, 249–302 (1969).
2. N. M. WHITE AND R. F. WING, *Astrophys. J.* **222**, 209–219 (1978).
3. K.-P. HUBER AND G. HERZBERG, "Constants of Diatomic Molecules," Van Nostrand–Reinhold, New York, 1979.
4. A. J. MERER, *Annu. Rev. Phys. Chem.* **40**, 407–438 (1989).
5. C. J. CHEETHAM AND R. F. BARROW, *Adv. High Temp. Chem.* **1**, 7–41 (1970).
6. S. R. LANGHOFF AND C. W. BAUSCHLICHER, JR., *Annu. Rev. Phys. Chem.* **39**, 181–212 (1988).
7. Y. M. HAMRICK, S. TAYLOR, AND M. D. MORSE, *J. Mol. Spectrosc.* **146**, 274–313 (1991).
8. A. G. ADAM, Y. AZUMA, J. A. BARRY, G. HUANG, P. J. LYNE, A. J. MERER, AND J. O. SCHRÖDER, *J. Chem. Phys.* **86**, 5231–5238 (1987).
9. V. I. SRDANOV AND D. O. HARRIS, *J. Chem. Phys.* **89**, 2748–2753 (1988).
10. B. ROSEN, *Nature (London)* **156**, 570 (1945).
11. D. W. GREEN, G. T. REEDY, AND J. C. KAY, *J. Mol. Spectrosc.* **78**, 257–266 (1979).
12. G. GUSTAFSSON AND R. SCULLMAN, unpublished report (1983).
13. M. J. MCQUAID, K. MORRIS, AND J. L. GOLE, *J. Am. Chem. Soc.* **110**, 5280–5285 (1988).
14. S. P. WALCH AND W. A. GODDARD, *J. Am. Chem. Soc.* **100**, 1338–1348 (1978).
15. C. W. BAUSCHLICHER, JR., C. J. NELIN, AND P. S. BAGUS, *J. Chem. Phys.* **82**, 3265–3276 (1985).

16. C. W. BAUSCHLICHER, JR., *Chem. Phys.* **93,** 399–409 (1985).
17. M. DOLG, U. WEDIG, H. STOLL, AND H. PREUSS, *J. Chem. Phys.* **86,** 2123–2131 (1987).
18. E. J. FRIEDMAN-HILL AND R. W. FIELD, *J. Mol. Spectrosc.* **155,** 259–276 (1992).
19. L. R. BROWN AND R. A. TOTH, *J. Opt. Soc. Am. B* **2,** 842–856 (1985).
20. J. M. BROWN, E. A. COLBOURN, J. K. G. WATSON, AND F. D. WAYNE, *J. Mol. Spectrosc.* **74,** 425–436 (1979).
21. C. R. BRAZIER, R. S. RAM, AND P. F. BERNATH, *J. Mol. Spectrosc.* **120,** 381–402 (1986).
22. U. SASSENBERG AND R. SCULLMAN, *Phys. Scr.* **28,** 139–159 (1983); *J. Mol. Spectrosc.* **68,** 331–332 (1983).
23. C. I. FRUM, R. ENGLEMAN, JR., AND P. F. BERNATH, *J. Mol. Spectrosc.* **150,** 566–575 (1991).
24. H. LEFEBVRE-BRION AND R. W. FIELD, "Perturbations in the Spectra of Diatomic Molecules," Academic Press, Orlando, FL, 1986.